Development of an Efficient Approach to Simulate Active Flow Control Methods for Interference Drag Reduction of a Strut-Braced Wing Configuration

Jan-Philipp Hofmann[1]
ILR, RWTH University, 52062 Aachen, Germany

In this work a zonal approach is developed to simulate Active-Flow-Control methods more efficiently. For this purpose, the flowfield around a Strut-Braced Wing Configuration in which strong shocks due to interferences between wing and strut occur is simulated by the DLR TAU-code. For the zonal approach a modular grid consisting of an inner module that encompasses the wing strut junction area and an outer module that covers the remaining flow field is generated in the grid generator CENTAUR. After a simulation of the entire flow field, the conservative flow variables on the module boundary are extracted and used for a sole simulation of a different inner module. This concept, the zonal simulation of a replaceable inner module, enables a fast integration and efficient simulation of Active-Flow-Control systems. To check the admissibility of the concept, the shock is weakened and the drag is reduced by Active-Flow-Control. Finally, a simulation of the entire flow field is used to check how accurate the zonal simulation reproduces the influence of the Active-Flow-Control system. The computing time benefit equals the ratio of the number of grid points of the inner module to the total number of grid points. The result of this work, conducted at the Institute of Aerodynamics and Flow Technology, German Aerospace Center, about 40 % of computation time could be saved by the developed concept.

Nomenclature

Ma	=	Mach number
p	=	Pressure
x_c	=	Coordinate in chord direction
y	=	Coordinate in wingspan direction
C_D	=	Drag coefficient
C_L	=	Lift coefficient
C_P	=	Pressure coefficient
v_{AFC}	=	jet velocity (Active Flow Control System)
WS	=	Workshop

I. Introduction

One objective of new aircraft configurations is to increase aerodynamic efficiency significantly. The potential of a Strut-Braced Wing (SBW) Configuration is to reduce the induced drag by increasing the aspect ratio of the wing. However, local flow phenomena occur and strong shocks in the junction area between wing and strut decrease the profits due to less induced drag considerably. The wave drag probably can be controlled by flow-control devices. Thus, an integrated design approach seems mandatory to estimate the real potential of the configuration. To simulate Active-Flow-Control (AFC) systems, a high spatial flow resolution is necessary. This results in a high computation effort. Therefore, AFC systems could not be considered in early design stages based on Reynolds-averaged Navier-Stokes equations (RANS) so far.

---

[1] Scientific Research Assistant, M. Sc., Institute of Aeronautics and Astronautics (ILR), RWTH Aachen University of Technology, Wüllnerstraße 7, 52062 Aachen, Germany.

The aim is to develop and assess an approach that allows a simplified simulation of the aerodynamic impacts of AFC systems. For this purpose, the flow will be simulated zonally, in a spatially limited area of the flow field. The significant reduction of the simulated flow field and the resulting reduction of grid points, for which the flow quantities must be calculated, promise a reduced computing time.

To achieve this, a modular grid consisting of an inner module that encompasses the previously defined limited area and an outer module that covers the remaining flow field is generated. The simulation results of the entire flow field allow to write out the flow state at the module boundary. These values are used as a boundary condition for the sole simulation of the inner module. The concept developed from this approach for an efficient simulation of the influence of AFC systems now enables the exchange and sole simulation of the inner module while maintaining the boundary conditions of the original module. Provided that the grid points on the module boundary coincide exactly, precautions for the installation of AFC systems can be integrated into the geometry and local refinements can be implemented.

The impact of AFC systems is first analysed within the inner module. Since this approach neglects the effects on the flow field outside this area, the entire flow field is finally simulated to check the result achieved for the inner module. If the results are consistent, this approach could allow the consideration of AFC systems in early design stages based on RANS. The expected benefit in computing time equals the ratio of the proportion of inner to total grid points.

II. SBW Configuration and potential AFC Systems

Since the early days of aircraft development, there has been the idea of supporting wings of an aircraft with struts on the fuselage to reduce wing root bending moment. While this construction method was broadly used at the beginning of the 20th century, its use declined with increasing aircraft size and higher flight speeds over time [1]. The use of thicker wing profiles and the development of better materials enabled self-supporting wings without drag-producing struts. Nowadays, braced wings can only be found on slow-flying small aircraft such as the Cessna Skyhawk. Nevertheless, the SBW concept is also interesting for commercial aircraft operating in the transonic speed range due to its enormous aspect ratio potential and is therefore the subject of many scientific studies. [2] - [13]

The investigated SBW Configuration is taken from the "Platform for Aircraft Drag Reduction Innovation" (PADRI) [14]. For the flow simulation with the focus on the junction area between wing and strut, a semi-model of the aircraft without engines and empennage, a compatible grid as well as the corresponding flow solution are provided. The Mach number, flight altitude and angle of attack are specified in addition to the fixed geometry.

The existing numerical flow solution is examined in more detail. Figure 1 shows an isosurface with $Ma = 1$, which provides an overview of the flow state around the semi-model.

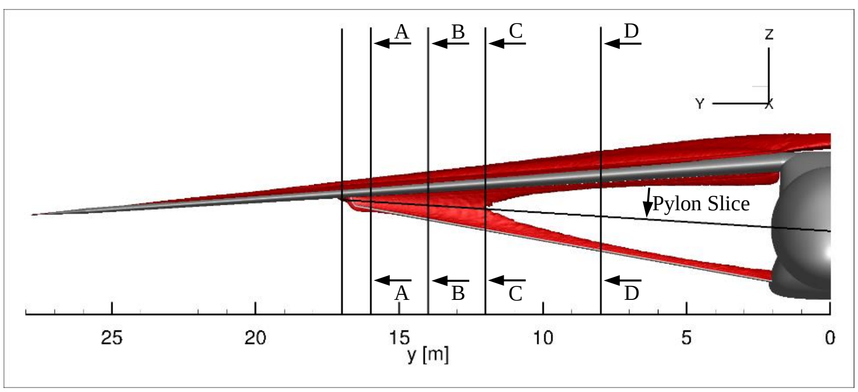

Figure 1 Dissemination of the supersonic flow

A large, connected supersonic area grows between wing and strut. According to previous research, the supersonic area due to interferences between strut and wing is caused by the almost two-dimensional nozzle-like geometry [6]. This becomes clear in Figure 2 where velocity distributions are shown for different spanwise positions (cf. Figure 1).

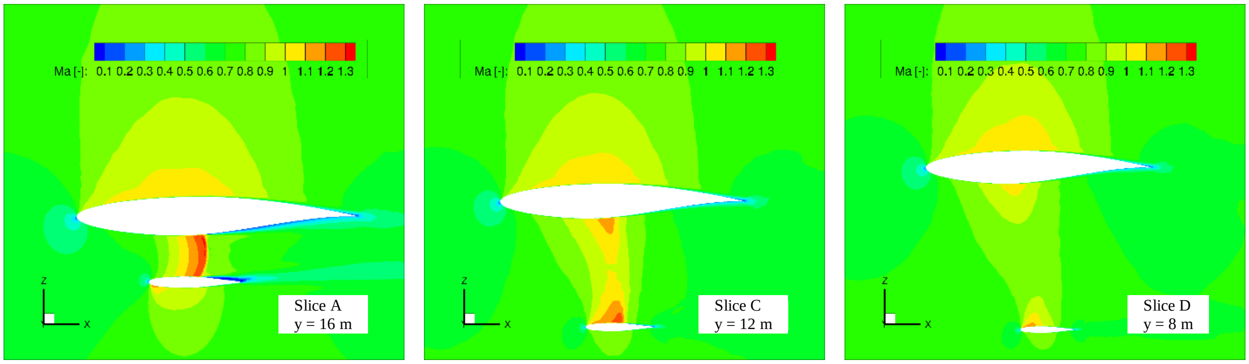

Figure 2 Velocity distribution between wing and strut

Far away from the pylon (y = 8 m) only small interferences are recognizable between wing and strut. With decreasing distance between wing and strut, the flow conditions change significantly. Close to the pylon (y = 16 m) the flow is accelerated which results in a strong vertical shock and large areas of separated flow downstream. These local flow phenomena are obviously responsible for the increased wave drag.

To weaken the shock and to influence the areas of separated flow, different possibilities are conceivable. If the nozzle-like contour between strut and wing is defused by flattening off one surface, preferably the upper side of the strut, the shock is significantly reduced [6]. Instead of a shape optimization, in this study it is supposed to reduce drag by an AFC system that has a visible influence on the flow. Three approaches in which AFC is implemented by constant blowing through slots in the strut are briefly presented below. Constant blowing is effective and can be solved with steady state simulations. Undoubtedly, the mass flux and consequently the efficiency could be improved by pulsed blowing, but this can be disregarded in this work, because neither an optimization of the AFC system nor an optimization of drag should be done. [15]

The easiest way to reduce drag could be a tangential blowing behind the shock to delay separations. However, this approach does not reduce the reason of the shock. To reduce the nozzle effect between strut and wing, the flow velocity in this area could be reduced by tangential blowing at outer sides of strut and pylon. Due to the resulting Supercirculation the stagnation line shifts and the strength of the shock is reduced. A method that might be slightly better recognizable is the creation of a Fluid Gurney-Flap. Perpendicular blowing close to the trailing edge reduces the cross-section between the (fluid) trailing edge of the strut and wing. Consequently, a reduction of mass flow is achieved, which implicates a slower maximum velocity in the smallest cross-section. The shock strength is reduced as a response. The geometry of the AFC system shown in Figure 3 is based on an AFLoNext design [15].

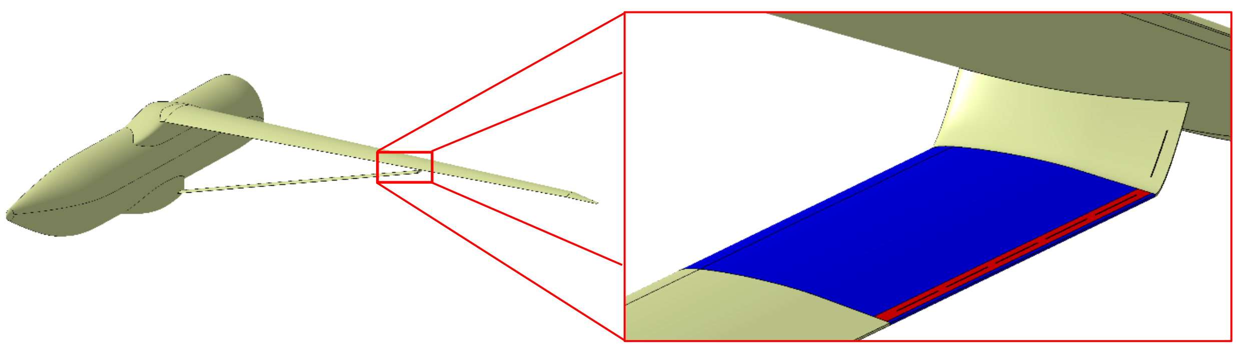

Figure 3 Integration of AFC system for Fluid Gurney-Flap

Multiple blowing slots are positioned on strut and pylon. By adopting the geometry parameters proposed by the results of AFLoNext, the slots were positioned at 95 % local chord length and with a width of 25 % local chord length. Maintaining these dimensions facilitates the concentration on the jet velocity in the presented investigation.

In order to assess the drag reduction and the influence of the AFC systems on the flow a modular grid is created in CENTAUR and the flow solution is solved by the unstructured compressible DLR flow solver TAU [16], [18]. In the present study the main flow equations are calculated by a second order upwind scheme. The equations of the one-equation Spallart-Allmaras turbulence model are also calculated by a second order upwind scheme [19], [20].

III. Approach for More Efficient RANS-Simulations of Local Flow Problems

To increase the efficiency of a numerical flow simulation with the zonal simulation approach, only a spatially limited area of the flow field is simulated. The repercussions on the flow field outside the inner module are neglected. In the present work, the examined area is the enclosed area between the wing and strut of the presented SBW Configuration.

Before a zonal simulation is possible, the entire flow field has to be simulated on a new modular grid. The grid consists of an inner module, which covers the previously defined area, and an outer module, which covers the remaining flow field. The new modular grid enables an efficient, finer resolution due to the use of structured elements on wing and strut as well as the variation of different settings. Moreover, the modular structure enables the exchange of the inner module while retaining the grid points on the module boundary. Finally, the flow field in the inner module is simulated individually. The reduction of the simulated flow field and the resulting reduction of grid points for which the flow quantities have to be calculated promises a reduced calculation time. It is expected that the computation benefit equals the ratio of the number of inner vs. total grid points. Following the zonal simulation, it is tested whether the flow within the module corresponds to that of the simulation of the entire flow field.

A. Generation of a Modular Grid

To enable modular mesh generation, the module boundaries between the inner and outer modules must be defined. The box shown in Figure 4 is constructed for this purpose. The vertical lateral interfaces of the box are positioned according to the supersonic area and aligned perpendicular to the wing and strut surfaces. All other surfaces, top and bottom as well as front and back, have been positioned in such a way that they enclose the area as tight as possible but at the same time have the least possible impact on the simulation results.

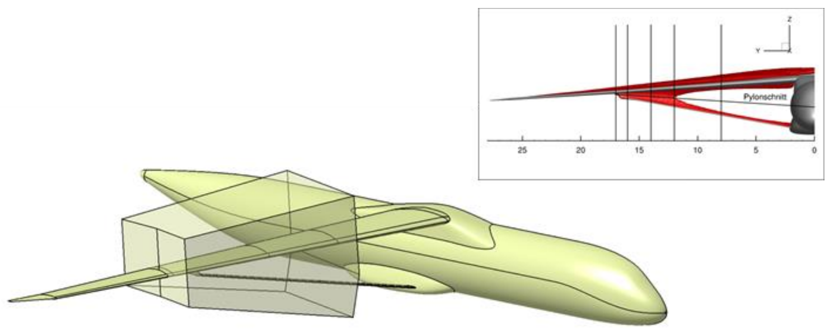

Figure 4 Constructions of module boundaries

After splitting the original model into an inner module and an outer module part, the grid generator CENTAUR is used to build up the new modular mesh. Structured elements on wing and strut surfaces enable a finer resolution in chord length while simultaneously the number of grid points can be reduced in spanwise direction. Moderate improvements are also made for an increased shock resolution. This is achieved with local refinements around the wing-strut-junction as shown in Figure 5.

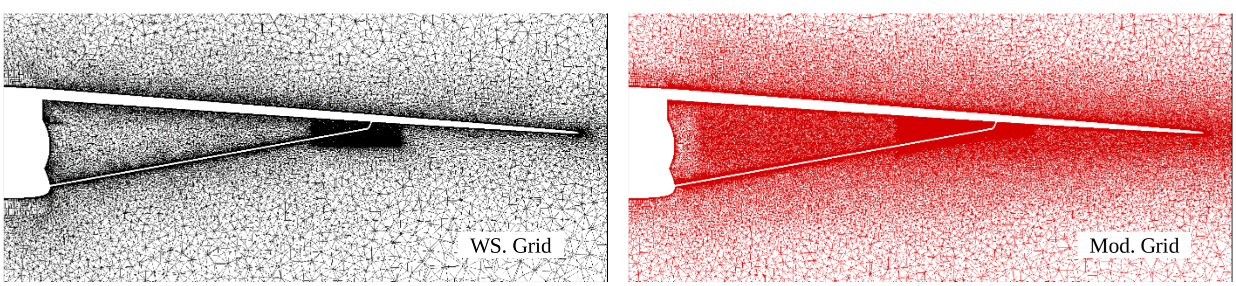

Figure 5 Comparison of grid resolution

Because of the finer resolution in the investigated area and the avoidance of significant changes in cell volume the shock can be precisely resolved. As seen in the right part of Figure 6 the shock extends in fuselage direction when using the modular grid. In the PADRI Workshop Grid (see right Part) the shock diffuses at coarser resolution.

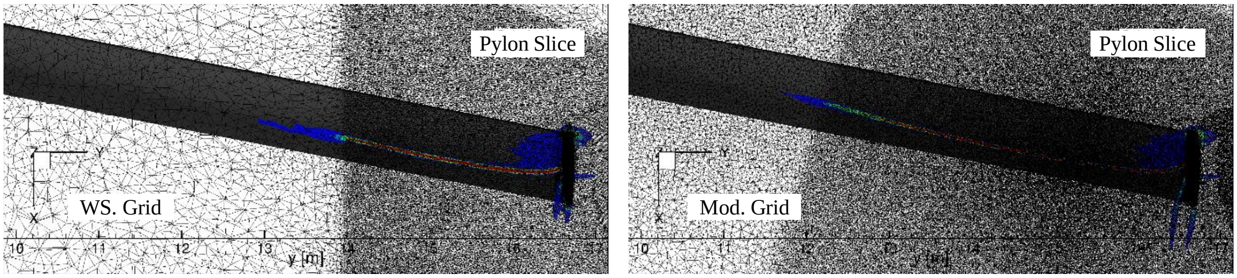

Figure 6 Comparison of shock resolution (colours by $\log(1+|\nabla\rho|)$)

This also affects the pressure distribution over chord length as shown in Figure 7. On the upper side of the strut and on the bottom side of the wing, the shocks in the Workshop Grid are much further upstream and weaker. Thus the statement, the shocks diffuse in the Workshop-Grid, is confirmed. The remaining pressure distributions are almost identical, especially on the upper wing and the bottom strut surfaces. The small pressure fluctuations, e.g., on the upper strut surface, are caused by non-optimized profiles [14].

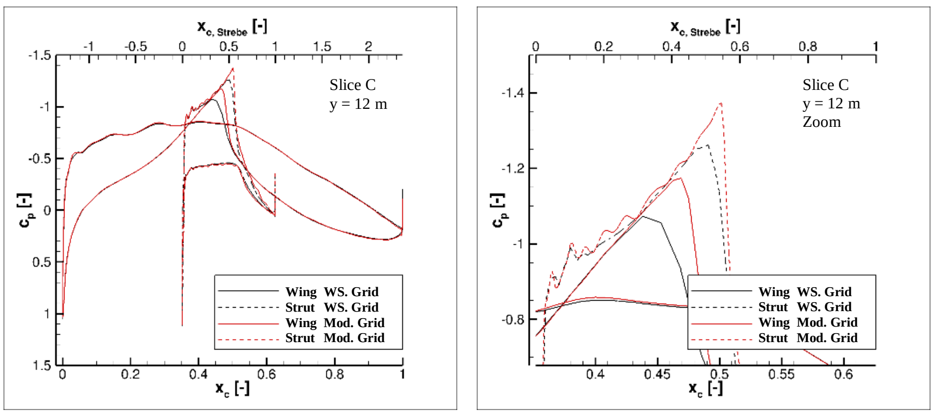

Figure 7 Comparison of shock resolution by pressure coefficient

It can be assumed that the new generated modular grid can achieve a more precise flow simulation. Even if it probably does not lead to a grid-converged solution, it is sufficiently suitable for the approach to increase the efficiency of a flow simulation developed in this work. The modular grid structure, as shown in Figure 8, not only allows the replacement of the inner module while retaining the nodes on the module boundary, but also a zonal simulation of the inner module.

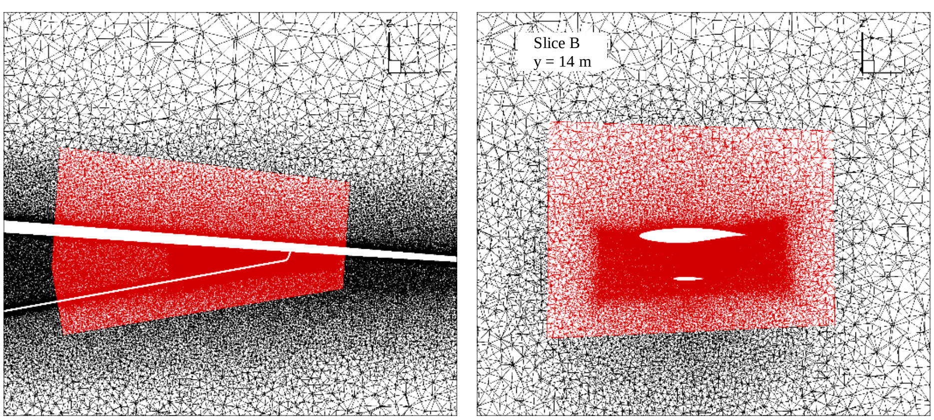

Figure 8 Modular grid generation

B. Zonal Simulation of the Basic Module

To enable zonal simulations the conservative flow variables on the boundary grid points have to be extracted (cf. Figure 9 a)) [21]. In contrast to other techniques such as "Chimera" or "Non-Matching Boundaries", the modular grid gives the opportunity to import the extracted values on the corresponding grid points with a modified farfield boundary condition.

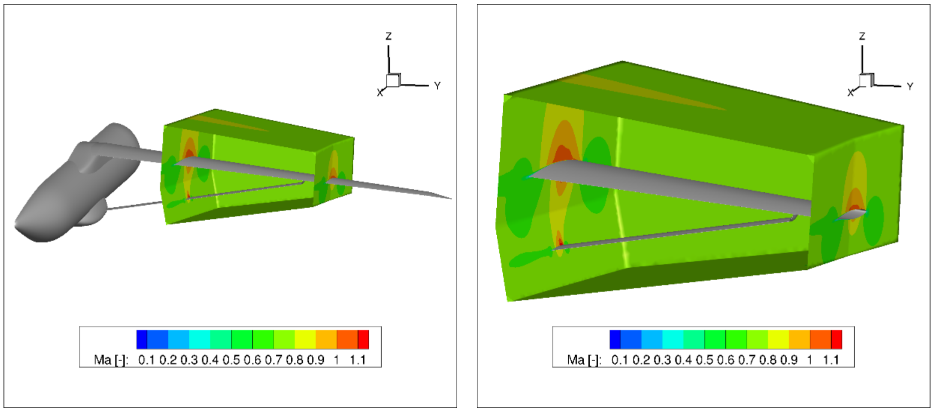

Figure 9 a) Extracted conservative flow variables b) Imported values for a zonal simulation

On the inflow, top, bottom and side faces the conservative variables are set as a Dirichlet boundary condition (cf. Figure 9 b)). Since in the further progress of this work AFC measures in the inner module are simulated, which inevitably entail a change of the total mass flow within the module limits, the flow variables may not be fixed on all surfaces of the module boundary. At least one face, preferably the outflow face should be defined as a normal farfield boundary condition. This results in characteristic outflow boundary conditions which allow the variation of some flow parameters and the additional mass flux of AFC systems can flow off. The flow field inside the module is initialized with free-stream values. With these settings different inner modules with matching grid points on the boundary can be simulated zonally.

In order to check whether the flow in the basic inner module is reproduced precisely enough with the zonal simulation approach it is simulated with the same numerical settings. The results of this zonal flow simulation can be easily compared with those results inside the module obtained from the simulation of the entire flow field. Figure 10 shows the deviation of the pressure coefficient from the zonal simulation of the basic module with respect to the entire simulation for $C_P > 0.005$.

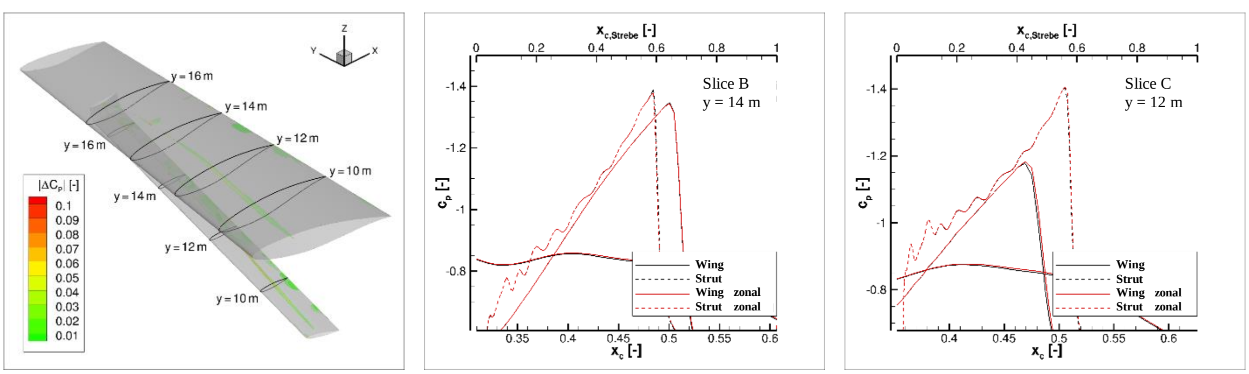

Figure 10 Comparison of zonal and entire simulation by pressure coefficient

Deviations of less than $C_P = 0.005$ are found over large parts of wing and strut. Larger deviations (max $C_P = 0.1$) can only be seen in two narrow stripes between y = 10 m and y = 14 m on the bottom side of the wing and the top of the strut. To take a closer look the pressure distribution is plotted for y = 14 m and y = 12 m. The larger differences of the pressure coefficient between entire and zonal simulation occur exactly at the shock position. Only in this area, a minimum displacement causes a larger pressure difference due to the high gradient of the pressure coefficient. The displacement is minimal so that it can be neglected in this work. Consequently the zonal simulation provides an accurate representation of the relevant effects in the local flow field. At the same time the simulation efficiency can be increased as expected. The benefit equals the ratio of the number of inner vs. total grid points.

IV. Application with a constant blowing AFC System

The concept pursued in this work is to combine the exchange of the inner module with zonal simulation while maintaining the grid points on the module boundary. The boundary conditions of the entire simulation with the base module are set to the module boundary of a deviating inner module. This allows to limit the simulation to an alternative internal module.

Next, the derived concept is tested by simulating the influence of the AFC system creating the Fluid Gurney-Flap. After the installation of the blowing slots in the inner module, local refinements are done to capture the AFC-jets. As seen in Figure 11 a huge amount of grid points is necessary for this.

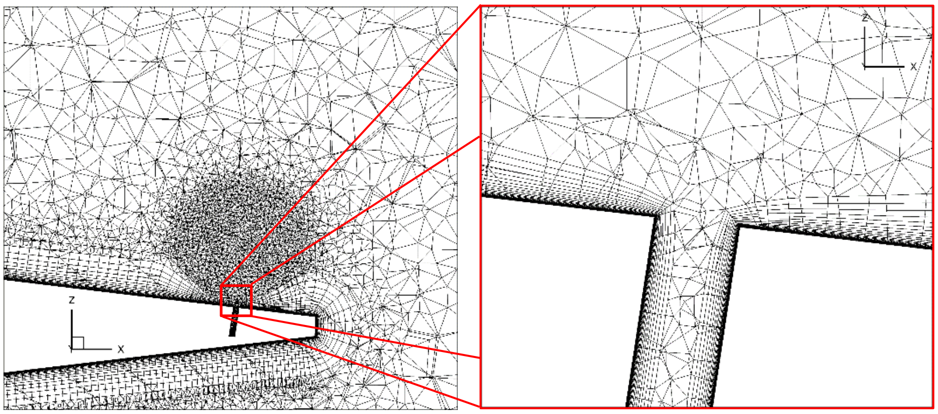

Figure 11 Mesh refinements to capture the AFC system

To test the derived concept of efficiently reproducing the influence of AFC systems through zonal simulation the jet velocity is adjusted in order to increase aerodynamic efficiency within the AFC Module. With increasing jet velocity, the drag is significantly reduced. This is shown in Figure 12, in which each black line specifies a constant lift to drag ratio.

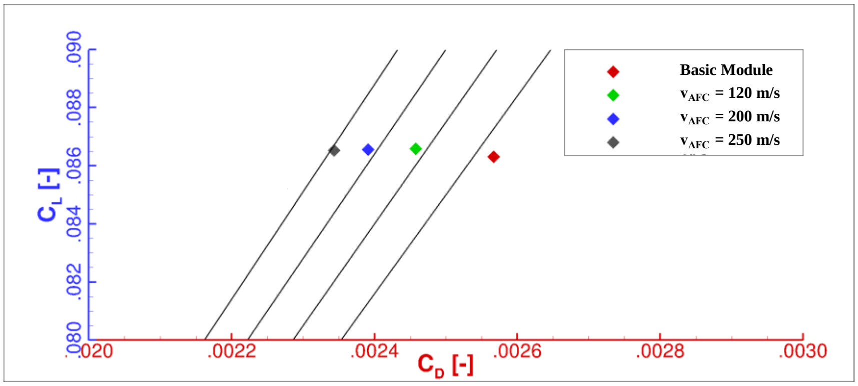

Figure 12 Influence of increasing jet velocity on drag coefficient

In the following section the flow simulation for the largest jet velocity with $v_{AFC} = 250\,\text{m/s}$ is examined in more detail. For this purpose, the velocity distribution of the Basic Module and the AFC Module as well as the corresponding pressure distributions are compared. Figure 13 shows the impact of the AFC system close to the pylon.

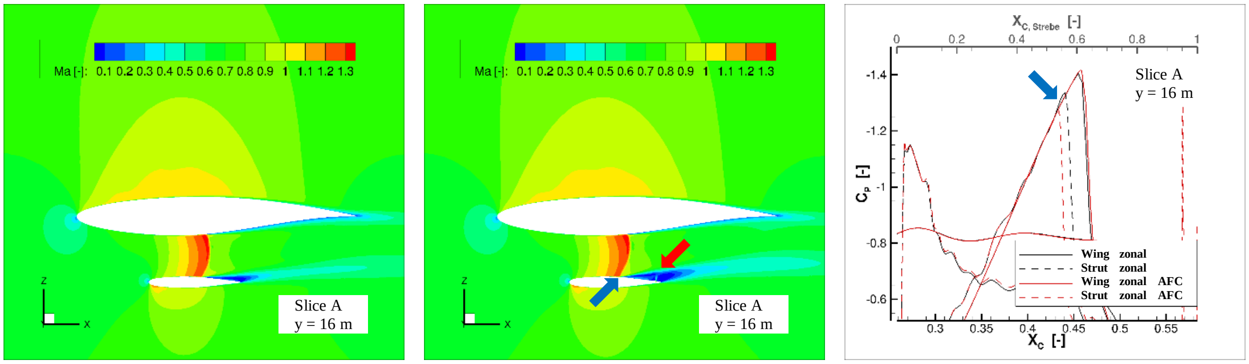

Figure 13 Comparison of Basic and AFC Module by velocity and pressure coefficient

The blowing and the desired effect, a Fluid Gurney-Flap, are clearly visible. As expected, the area of separated flow on the upper side of the strut increases. The rear edge of the supersonic area and thus the shock moved upstream on the strut. At the same time, the extent of the area with flow velocities greater than Ma = 1.3 decreases. As seen in the pressure distribution in the right part of Figure 13, the shock on the strut is weaker and more upstream.

Even at greater distance from the pylon, the Fluid Gurney-Flap and the desired effect can be seen (cf. Figure 14).

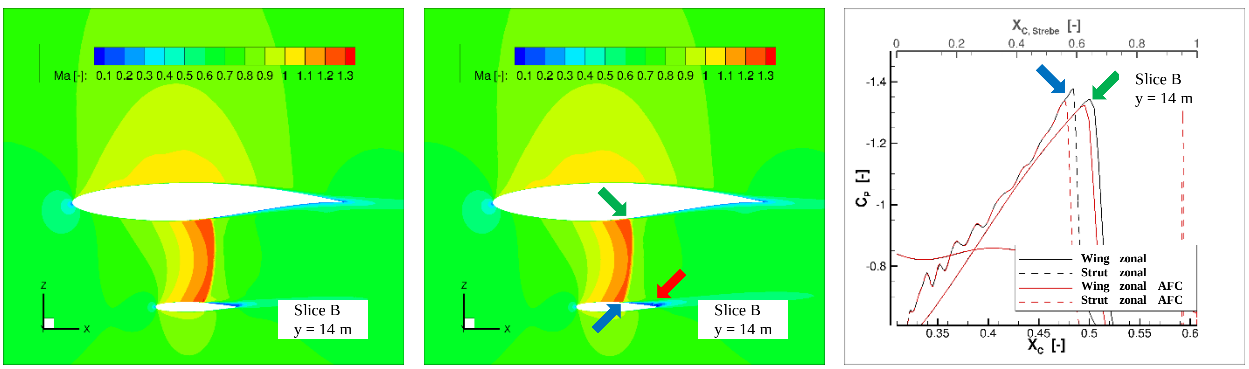

Figure 14 Comparison of Basic and AFC Module by velocity and pressure coefficient

The area of maximum velocity has decreased significantly. On wing and strut the shock location has moved upstream and the strength is reduced. In Figure 15 the location of the shock in the slice centrally between wing and strut (cf. Figure 1) is shown. Also in the middle between wing and strut the shock is weaker and further upstream.

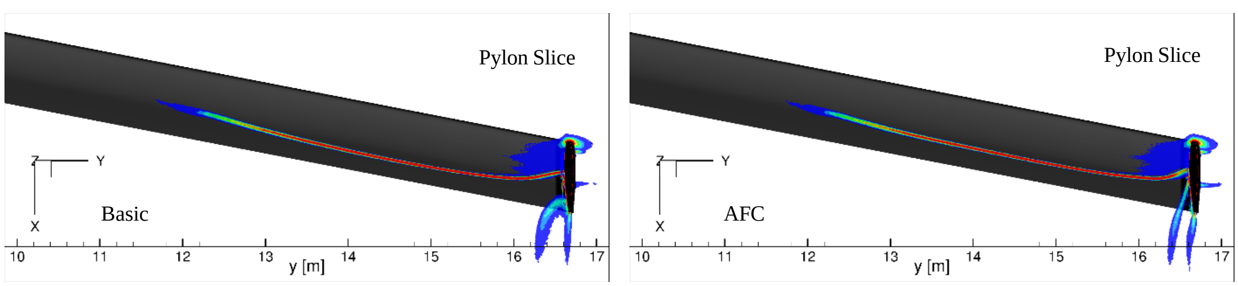

Figure 15 Comparison of shock resolution (colours by $\log(1+|\nabla\rho|)$)

In summary the shock has been pushed upstream by the AFC system in the entire area under consideration. In the area of the AFC system, a significant shock reduction was also achieved. Even outside of the application of the AFC system, a slight weakening of the shock on the wing could be achieved. The drag coefficient within the module has thus been reduced by 2.2 drag counts, increasing aerodynamic efficiency by almost 10 %. It is expected that the reduction of the drag coefficient by 2.2 drag counts is transferable to the simulation of the semi-model in the entire flow field, and thus an increase in aerodynamic efficiency of just under 2 % could be achieved.

V. Verification of the concept

In order to test the extent to which the results of the zonal simulation of the AFC Module with the boundary conditions of the Basic Module can be transferred to the results of the simulation of the entire flow field, the entire flow field is simulated with a jet velocity of $v_{AFC} = 250\,m/s$. The drag reduction of 2.2 drag counts in the zonal simulation is exceeded by 2.58 drag counts in the entire simulation. This is due to the fact that the effects outside the inner module are neglected by the zonal simulation. The differences inside the module are shown by the deviations of the pressure coefficient in Figure 16.

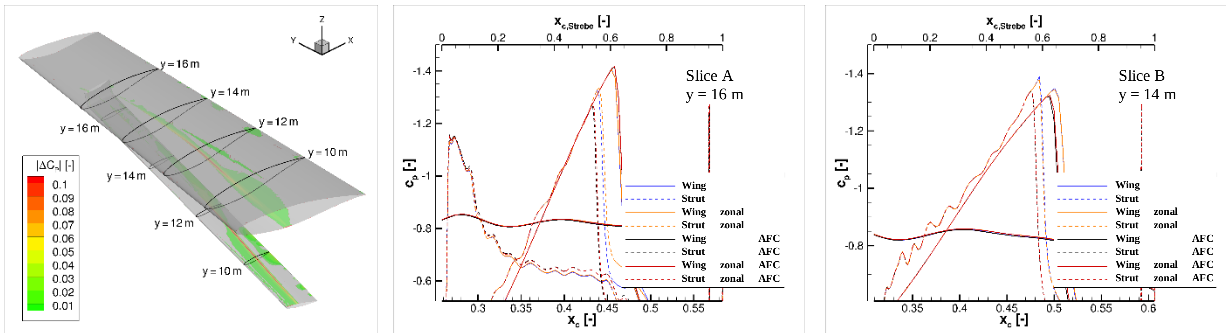

Figure 16 Comparison of zonal and entire simulation of the AFC Module by pressure coefficient

The zonal simulation enables a precise determination of shock location and strength in the area of the AFC system. Even in a greater distance from the pylon, the AFC dominates the effect of the boundary condition. Until $y = 13\,m$, the influence of the AFC system significantly exceeds the deviations due to the zonal simulation on the shock position and strength. Further away the small displacement of the two unconnected shocks on the upper strut and lower wing surfaces is no longer adequately represented by the zonal simulation. This is due to the fixed boundary conditions, in particular the defined shock position of the Basic Module and explains the difference in drag reduction between zonal and overall simulation.

In order to test the influence of the fixed flow state at the boundaries, the deviations of the flow quantities between the zonal and the entire simulation of the AFC Module at the module boundary are compared. Furthermore, based on the deviations of the conservative flow variables on the module boundary, it is possible to predict whether the inner module was sufficiently large. Figure 17 shows the percentage deviation of the pressure coefficient at the module boundary for $|\Delta p| > 0.1\,\%$.

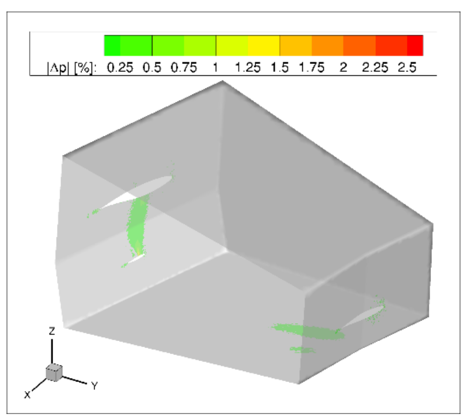

Figure 17 Comparison of zonal and entire Simulation of the AFC Module by deviations at the boundary

The deviations of the pressure coefficient are below 0.1 % almost on the entire module boundary. A larger deviation can only be seen as a narrow strip between wing and strut on the inside of the module boundary. Those deviations are based on the minimal displacement of the shock by the entire simulation of the AFC system. In order to represent this a big enlargement of the inner module until the fuselage would be necessary. However, since this would significantly reduce the efficiency achieved by zonal simulation and the flow is well represented in the direct influence area of the AFC system, a suitable compromise seems to have been found.

The increase in simulation efficiency can be determined on the basis of calculation times required for the simulations. Due to the zonal simulation, the computing time for the AFC Module is reduced by almost 40 %. The benefit in calculation times correlates with the number of grid points, so that the increase in efficiency through zonal simulation depends mainly on the size of the inner module. To estimate the potential of zonal simulations it must be taken into account that the entire flow field for the base module must be simulated before the zonal simulation of the AFC Module. Therefore, the zonal simulation approach will show its true potential when different AFC Modules are compared using the same module boundaries and the remaining flow field is only meshed and simulated once.

VI. Conclusion and Outlook

In this work, a concept was developed that allows efficient simulation of AFC systems to reduce the interference drag of a SBW Configuration. For this purpose, the approach of zonal simulation of the flow field has been chosen, in which changes in the flow are only investigated within a limited area. First of all, it has been shown that in the zonal simulation of the Basic Module, the shock pattern and strength are sufficiently consistent.

Subsequently the developed concept of exchanging the inner module and its zonal simulation while maintaining the boundary conditions of the previous module has been applied to an exemplary AFC system. For this purpose, an AFC Module was designed to create a Fluid Gurney-Flap, which was meshed in such a way that all grid points on the module boundary correspond to those of the Basic Module. The influence of the AFC system was examined and the aerodynamic efficiency was raised by increasing the jet velocity. The comparison of the flow field in the zonal simulation with the solution of the entire flow field showed that the displacement and the weakening of the shock within the range of the AFC system are predicted very precisely.

The developed concept already achieved a benefit of 40 % in computing time. It is conceivable that an optimization of the module boundary geometry yields to further advantages. If the results of this work are confirmed in further research, the developed concept can be used for a first evaluation of different positions as well as jet velocities and angles of AFC systems in early design stages based on RANS.

VII. Acknowledgements

The presented work was carried out as a part of the research project PADRI. I would like to extend my gratitude to my supervisors Prof. Eike Stumpf, Anna Uhl (Institute of Aerospace Systems, RWTH Aachen) and Niko Bier (Institute of Aerodynamics and Flow Technology, German Aerospace Center). Their supervision has been a great support and I am gratefully indebted for their involvement in my work.

References

[1] Bölkow, L.: Ein Jahrhundert Flugzeuge, Geschichte und Technik des Fliegens, Springer 1990

[2] Grassmeyer, J: Multidisciplinary Design Optimization of a Transonic Strut-Braced Wing Aircraft, AIAA Paper 1999-0010.

[3] Gern, F.H., Naghshineh-Pour, A.H., Sulaeman, E. und Kapania, R.K.: Flexible Wing Model for Structural Sizing and Multidisciplinary Design Optimization of a Strut-Braced Wing, AIAA Paper 2000-1327.

[4] Tétrault, P.-A.: Numerical Prediction of the Interference Drag of a Streamlined Strut Intersecting a Surface in Transonic Flow, Dissertation, Virginia Polytechnic Institute and State University, 2000.

[5] Gundlach, J.F., Tétrault, P-A., Gern, F., Nagshineh-Pour, A., Ko, A., Schetz, J.A., Mason, W.H., Kapania, R., Grossman, B. und Haftka, R.T.: Multidisciplinary Design Optimization of a Strut-Braced Wing Transonic Transport, AIAA Paper 2000-0420.

[6] Ko, A., Mason, W.H., Grossman, B. und Schetz, J.A.: A-7 Strut Braced Wing Concept Transonic Wing Design VPI-AOE-275, NASA PO #L-14266, 2002.

[7] Gern, F.H., Ko, A. Y-Y., Grossman, B., Haftka, R.T., Kapania, R.K., Mason, W.H., und Schetz, J.A.: Transport Weight Reduction Through MDO: The Strut-Braced Wing Transonic Transport, AIAA Paper 2005-4667.

[8] Bradley, M.: Subsonic Ultra Green Aircraft Research, NASA N+3, Final Review April 2010

[9] Gur, O., Mason, W. H., und Schetz, J.A.: Full Configuration Drag Estimation, Journal of Aircraft, Vol. 47, No. 4, S. 1356–1367, 2010.

[10] Ting, E., Reynolds, K., Nguyen, N. und Totah, J.: Aerodynamic Analysis of the Truss-Braced Wing Aircraft; Using Vortex-Lattice Superposition Approach, NASA 2014.

[11] Knight, K., Braun, E., Roy, C., Lu, F., und Schetz, J.A.: Interference Drag Modeling and Experiments for a High-Reynolds-Number Transonic Wing, Journal of Aircraft, Vol. 49, No. 6, S. 1894–1903, 2012.

[12] Duggriala, R.K., Roy, C.J. und Schetz, J.A.: Analysis of Interference Drag for Strut–Strut Interaction in Transonic Flow, AIAA Journal, Vol. 49, No. 3, 2011.

[13] Bradley, M.K. und Droney, C.K.: Subsonic Ultra Green Aircraft Research: Phase 2 – Volume 2 – Hybrid Electric Design Exploration, Boeing Research and Technology, Huntington Beach, California, 2015.

[14] PADRI, Platform for Aircraft Drag Reduction Innovation, 05/2017: www.aerospace-europe.eu.

[15] Brunet, V., Dandois, J., Verbeke, C.: Recent Onera Flow Control Research on High-Lift Configurations, Aerospace Lab: Issue 6, June 2013.

[16] AFLoNext-Projekt: WP5.1.1, Numerical Benchmark Data Description, November 2013, http://www.aflonext.eu.

[17] CENTAUR 11.6, for more Information visit http://www.centaursoft.com

[18] Gerhold, T.:Overview of the Hybrid RANS Code TAU – Numerical Flow Simulation for Aircraft Design, 2005.

[19] Spallart, P.R. und Allmaras, S-R.: A One-Equation Turbulence Model for aerodynamic Flows, AIAA Paper 1992-0439.

[20] NASA Langley Research Center, Turbulence Modeling Resource: https://turbmodels.larc.nasa.gov/

[21] Schlichting, H und Gersten, K: Grenzschicht Theorie, Berlin/Heidelberg, Springer 1997.